

Reconstructing Cosmic Peculiar Velocities from the Mildly Nonlinear Density Field

Andrzej Kudlicki, Michał Chodorowski, Tomasz Plewa and Michał Różyczka

N. Copernicus Astronomical Center, Bartycza 18, 00-716 Warsaw, Poland

9 February 2018

ABSTRACT

We present a numerical study of the cosmic density vs. velocity divergence relation (DVDR) in the mildly non-linear regime. We approximate the dark matter as a non-relativistic pressureless fluid, and solve its equations of motion on a grid fixed in comoving coordinates. Unlike N-body schemes, this method yields directly the volume-averaged velocity field. The results of our simulations are compared with the predictions of the third-order perturbation theory (3PT) for the DVDR. We investigate both the mean ‘forward’ relation (density in terms of velocity divergence) and the mean ‘inverse’ relation (velocity divergence in terms of density), with emphasis on the latter. On scales larger than about 20 megaparsecs, our code recovers the predictions of 3PT remarkably well, significantly better than recent N-body simulations. On scales of a few megaparsecs, the DVDR predicted by 3PT differs slightly from the simulated one. In particular, approximating the inverse DVDR by a third-order polynomial turns out to be a poor fit. We propose a simple analytical description of the inverse relation, which works well for mildly non-linear scales.

Key words: cosmology: theory – cosmology: dark matter – large-scale structure of the Universe – methods: numerical

1 INTRODUCTION

It is now widely believed that the large-scale structure formed by the growth of small inhomogeneities present in the early Universe. In this scenario, commonly referred to as the *gravitational instability* (GI) paradigm, cosmic density and velocity fields are tightly coupled, and the relation between them involves the cosmological parameter Ω . In the linear regime, i.e. for the r.m.s. density fluctuations much smaller than unity, the density–velocity divergence relation (DVDR) reduces to

$$\delta(\mathbf{r}) = -f^{-1}(\Omega, \Lambda) \nabla \cdot \mathbf{v}(\mathbf{r}). \quad (1)$$

Here, δ is the mass density fluctuation field, \mathbf{v} is the peculiar velocity field, distances are expressed in units of km s^{-1} , and

$$f(\Omega, \Lambda) \simeq \Omega^{0.6} + \frac{\Lambda}{70} \left(1 + \frac{\Omega}{2}\right) \quad (2)$$

(Lahav et al. 1991). The factor f depends mainly on Ω and only weakly on the cosmological constant Λ (provided that Λ is in the range allowed by observations). The comparisons between density and velocity fields are a useful test of the GI hypothesis. In principle, they may also be used as a tool to measure Ω (Dekel et al. 1993).

However, there is both theoretical (e.g., Kaiser 1984; Davis et al. 1985; Bardeen et al. 1986; Dekel & Silk 1986; Cen & Ostriker 1992; Kauffmann, Nusser & Steinmetz 1997;

Blanton et al. 1998; Dekel & Lahav 1998) and observational (e.g., Davis & Geller 1976; Dressler 1980; Giovanelli, Haynes & Chincarini 1986; Santiago & Strauss 1992; Loveday et al. 1996; Hermit et al. 1996; Guzzo et al. 1997; Giavalisco et al. 1998; Tegmark & Bromley 1998) evidence that galaxies are biased tracers of the matter distribution. As a result, the comparisons between the fields in question within linear theory cannot yield an estimate of Ω itself. What is actually measured is the quantity $\beta \equiv \Omega^{0.6}/b$, where b is the linear bias parameter.

The current state of estimates of β is confused. The so-called velocity–velocity comparisons generally result in low values of β ($\simeq 0.5$: Roth 1994; Schlegel 1995; Schaya, Peebles & Tully 1995; Davis, Nusser & Willick 1996; da Costa et al. 1997; Riess et al. 1997; Willick et al. 1997; Willick & Strauss 1998), while density–density comparisons yield high values ($\simeq 1.0$: Dekel et al. 1993; Hudson et al. 1995; Sigad et al. 1998). In velocity–velocity comparisons, galaxy density field is used to predict the associated peculiar velocity field, which in turn is compared to the observed peculiar velocities of a sample of galaxies with measured redshift-independent distances. In density–density comparisons, velocity data are used to reconstruct the underlying mass density field, in order to compare it with an observed galaxy density field. A number of possible explanations of the divergence in the

estimated values of β has been proposed (see, e.g., Sigad et al. 1998). One of them are non-linear effects.

The density fluctuations obtained from current redshift surveys (e.g. Fisher et al. 1994) and from the POTENT (Dekel et al. 1998) reconstruction of the mass density field slightly exceed the regime of applicability of linear theory. For example, the density contrast in regions like the Great Attractor or Perseus-Pisces is around unity even when smoothed over scales of 1200 km s^{-1} , currently employed in density–density comparisons (Sigad et al. 1998). In velocity–velocity comparisons, the fields in question are generally smoothed over smaller scales than in density–density ones. Astonishingly, while in current density–density comparisons the non-linear corrections to the linear density–velocity relation, equation (1), are accounted for, in velocity–velocity comparisons they are not. The only exception is an attempt by Willick et al. (1997) to model the DVDR by a second-order formula.* To their surprise, the maximum-likelihood fit of the predicted to the observed peculiar velocities was for zero amplitude of the second-order corrective term. However, the smoothing scale they used was $3 \text{ h}^{-1} \text{ Mpc}$. At such a small scale, the variance of the density field is already in excess of unity and, as we will show later, neither the linear nor the second-order formula is a good description of the actual DVDR.

The purpose of this paper is to propose a simple and accurate description of the DVDR at mildly non-linear† scales, which would be easy to implement in current velocity–velocity comparisons. To date, there have been several attempts to construct a mildly non-linear extension of relation (1). They were either based on various analytical approximations to non-linear dynamics (Bernardeau 1992; Catelan et al. 1995; Chodorowski 1997; Chodorowski & Lokas 1997, hereafter CL97; Chodorowski et al. 1998, hereafter CLPN), or N-body simulations (Mancinelli et al. 1994; Ganon et al., in preparation), or both (Nusser et al. 1991; Gramann 1993; Mancinelli & Yahil 1995). So far, the most comprehensive description of the mildly non-linear DVDR has been recently done by Bernardeau et al. (1999; hereafter B99). Our work is an extension and improvement of B99 in several ways:

- In B99 the analysis was for technical reasons performed solely for fields smoothed with a top-hat filter. Here we also analyze fields smoothed with a Gaussian filter, which is now commonly applied to observational data.
- The fully non-linear formula proposed by B99 expresses density in terms of the velocity divergence (the so-called ‘forward’ relation). However, in velocity–velocity comparisons one needs a formula for the velocity (divergence) expressed as a function of the density (the so-called ‘inverse’ relation). Due to the scatter in the DVR, the latter is not given by a

* Strictly speaking, they proposed a fully non-linear formula, but in the process of actual comparison they truncated it at second order terms.

† We define mildly non-linear scales as these at which the r.m.s. density fluctuation is a significant fraction of, but still smaller than, unity. Then the mildly non-linear scales in the Universe are about or greater than $8 \text{ h}^{-1} \text{ Mpc}$ for top-hat smoothing, and roughly twice smaller for Gaussian smoothing.

straightforward inversion of the former. We obtain such an ‘inverse’ formula here.

- Our ‘inverse’ formula is much simpler compared to the ‘forward’ one of B99, but equally accurate, as detailed comparisons with numerical simulations show. Unlike the second order formula used by Willick et al. (1997), it works well for smoothing scales down to a few megaparsecs.

- Instead of performing N-body simulations, we model cold dark matter as a pressureless cosmic fluid. We solve non-linear equations for its evolution on a grid fixed in co-moving coordinates. This approach is advantageous over the standard N-body one for studying the evolution of the *velocity* field in the mildly non-linear regime. The reasons are outlined below.

Both in N-body simulations and in our code, the final velocity field is known at a discrete set of points. In the case of an N-body simulation this set is particles’ positions, in our case it is the grid. Due to clustering, the N-body velocity field is sampled very non-uniformly, while the sampling of our velocity field is perfectly uniform. Smoothing of a non-uniformly sampled velocity field leads to the so-called ‘sampling gradient bias’ (Dekel, Bertschinger & Faber 1990). In N-body simulations, the sampling rate of the velocity field is proportional to the number density of particles in a given region. The averaging of the field within a smoothing window is therefore not volume- but mass-weighted, resulting in a special type of bias mentioned above. To circumvent this problem, elaborate ‘tessalation’ algorithms for the velocity field have been proposed (Bernardeau & van de Weygaert 1996). However, they work only for a top-hat filter. Another problem is that N-body simulations provide very little information on the velocity field in voids, simply because there are very few velocity tracers there.

Due to uniform sampling, our simulations yield directly volume-weighted values of velocity, for any type of smoothing. Moreover, we probe the velocity field in the voids as finely as in dense regions. As a result, at a very low numerical cost it was possible to have the velocity field sampled at a comparable number of points to that of B99 (64^3 compared to 50^3), and still of significantly better quality, as shown below.

The paper is organized as follows: In Section 2 we discuss the theoretical aspects of the DVDR. Then, in Section 3, we present our simulations, describing the algorithm in Section 3.1 and the cosmological model investigated in Section 3.2. In Section 4 we investigate the mean forward density–velocity relation and we demonstrate that it is well described by a third-order polynomial. In Section 5.1 we show that the polynomial formula is a poor approximation of the *inverse* relation, and we propose an alternative description in Section 5.2. We summarize our results in Section 6.

2 THEORETICAL FRAMEWORK

Due to the Kelvin circulation theorem, the cosmic velocity field remains irrotational before shell-crossings. It can therefore be described by a single scalar function, which we choose here to be the velocity divergence, $\nabla \cdot \mathbf{v}$ (throughout the paper the derivative is taken in velocity units, i.e.

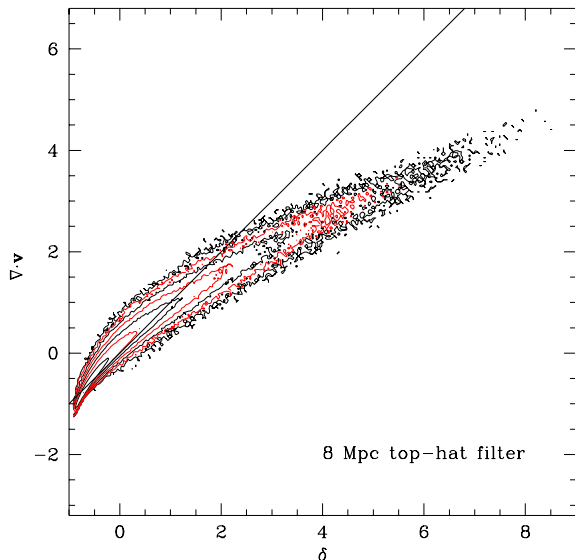


Figure 1. Joint probability distribution function of density and velocity divergence, $P(\delta, \nabla \cdot \mathbf{v})$, from a 64^3 simulation. Data are convolved with a $8h^{-1}\text{Mpc}$ top-hat filter. Contours have intervals of 0.5 in $\log_{10}(P)$. Solid line represents the linear relation.

$H = 1$). The linear relation (eq. 1) between the density contrast and the velocity divergence at a given point holds only on scales large enough so that the density fluctuations are much smaller compared to unity. On smaller scales, non-linear effects modify the relation in a number of ways. For full discussion of the density versus velocity divergence relation in the mildly non-linear regime the reader is referred to B99.

In brief, qualitative features of the relation can be outlined as follows:

- It is non-linear.
- It is also non-local, which implies that it is locally non-deterministic, i.e. it has a scatter in δ for a given $\nabla \cdot \mathbf{v}$ and vice versa.
- Since the scatter originates exclusively from higher (than linear) order terms, it is small in the mildly non-linear regime. Therefore, the most probable values of δ and $\nabla \cdot \mathbf{v}$ form an elongated region in the $(\delta, \nabla \cdot \mathbf{v})$ plane.

Figure 1 is a typical plot of the values of δ and $\nabla \cdot \mathbf{v}$ obtained in our simulations. The fields are smoothed with a top-hat filter with the smoothing radius of $8h^{-1}\text{Mpc}$. For such a smoothing scale, the r.m.s. fluctuation of the density field, σ_δ , in our simulations is $\simeq 0.9$, so the fields are close to leave the regime of mild non-linearities. However, in Figure 1 one can still observe an obvious correlation between the density and velocity divergence.

Analytical calculations predict (Bernardeau 1992; Gramann 1993; Catelan et al. 1995; Mancinelli & Yahil 1995; Chodorowski 1997; CL97; CLPN) and N-body numerical simulations confirm (Mancinelli et al. 1994; B99; Ganon et al. 1999) that the mildly non-linear DVDR depends on Ω and Λ in a very simple way. Specifically, if we define the *scaled* velocity divergence,

$$\theta \equiv -f^{-1}(\Omega, \Lambda) \nabla \cdot \mathbf{v}, \quad (3)$$

the relation between the density and the scaled divergence (for simplicity it will also be referred to as DVDR) will be practically Ω - and Λ -independent. Since the relation has a scatter, the full information about the DVDR is contained in the joint probability distribution function (PDF) for δ and θ . Such a joint PDF has been constructed by B99. However, the scatter is small compared to random errors in the observed density and velocity fields (CLPN). Therefore, of most interest for practical applications are the mean relations: the mean density for the given velocity divergence, $\langle \delta | \theta \rangle$ (the ‘forward’ relation), and vice-versa, $\langle \theta | \delta \rangle$ (the ‘inverse’ relation).[‡] The forward relation is relevant for density–density comparisons; the inverse relation is relevant for velocity–velocity comparisons. Since velocity–velocity comparisons employ smaller smoothing lengths, non-linear effects are more important there than in density–density comparisons. That is why in this paper we shall concentrate on finding a simple, and simultaneously robust, description of the inverse relation for Gaussian smoothing of the fields.

Though one might formally derive the inverse relation from the joint PDF constructed by B99, it would be inappropriate for a number of reasons. Firstly, while the forward relation can be derived from this PDF in an analytic form, the inverse one can only be computed numerically. Secondly, the joint PDF was constructed by B99 for top-hat smoothed fields and it is expected to depend quantitatively on the type of smoothing. Finally, with our fluid code we hope to trace the actual DVDR more accurately.

The mildly non-linear regime is the one in which perturbation theory can be applied. In particular, the mean relations are a priori accessible to analytical perturbative calculations. CL97 derived the forward DVDR up to third-order terms, accounting for the smoothing of the density and velocity fields. The mean density contrast given the scaled velocity divergence is a third-order polynomial in the divergence,

$$\langle \delta | \theta \rangle = a_0 + a_1 \theta + a_2 \theta^2 + a_3 \theta^3, \quad (4)$$

where $a_0 = -a_2 \sigma_\theta^2$ and σ_θ^2 is the variance of the scaled velocity divergence field, $\langle \theta^2 \rangle$. The coefficients, a_i , appearing in the above expansion were explicitly calculated by CL97 for Gaussian smoothing and by B99 for top-hat smoothing. As explained above, they depend extremely weakly on Ω and Λ . CLPN derived the inverse relation up to third-order terms,

$$\langle \theta | \delta \rangle = r_0 + r_1 \delta + r_2 \delta^2 + r_3 \delta^3. \quad (5)$$

The coefficients r_i were calculated by CLPN for Gaussian smoothing and by B99 for top-hat smoothing.

Contributions to the DVDR from orders higher than third are known in only one special case, of unsmoothed fields with vanishing variance. Bernardeau (1992) derived for this case the following formula:

$$\langle \theta | \delta \rangle = \frac{3}{2} [(1 + \delta)^{2/3} - 1]. \quad (6)$$

The above expression is strictly valid only for $\sigma_\delta \rightarrow 0$ and $\Omega \rightarrow 0$, but since the Ω -dependence of the (scaled) DVDR

[‡] Due to the scatter, the inverse relation is not given by a straightforward inversion of the forward one.

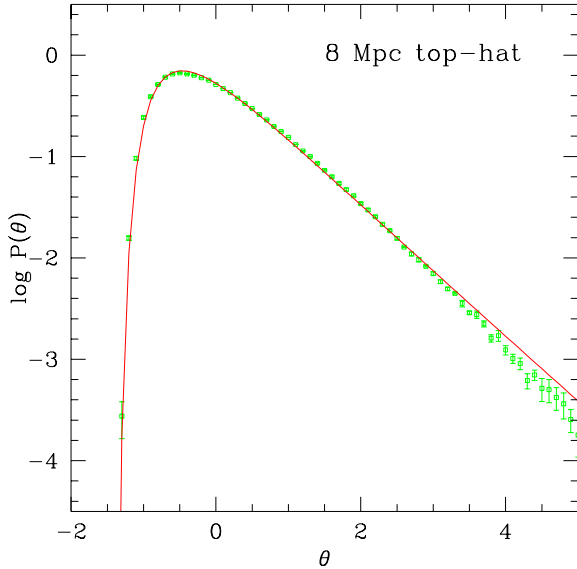


Figure 2. $P(\theta)$, the probability distribution of the scaled velocity divergence for $8h^{-1}\text{Mpc}$ top-hat smoothing. Open squares are combined results from our six runs, with error-bars shown. Solid line represents formula (12) of Bernardeau (1994), with the variance of θ taken to be the average from our simulations.

is extremely weak, it remains a good approximation also for other values of Ω .

Equations (5) and (6) are two different approximations to the inverse relation. As already stated, equation (5) accounts for smoothing and for finite variances of the fields. Equation (6) does not,[§] but instead it includes contributions from all orders. We can therefore expect the two equations to carry complementary information about the actual relation. Our procedure of finding a simple and accurate description of the inverse relation will consist of two steps. Firstly, we will check on which scales the third-order expression (5) is a good description of the relation, and at which scales it already fails. Then, guided by our numerical results, and by equation (6), we will look for a formula for the inverse relation, which would be accurate in the whole range of the mildly non-linear scales.

3 THE SIMULATIONS

3.1 The code

As stated in Section 1, despite their simplicity and numerous advantages, N-body simulations of cosmic velocity fields have several drawbacks.

To cope with them, we have performed our simulations using *CPPA* (Cosmological Pressureless Parabolic Advection): our original Eulerian, uniform-grid based code for self-gravitating pressureless fluid evolution in an expanding Universe. The main ideas of the algorithm are similar to those

of Peebles (1987), with several modifications. An early version of the code is described in Kudlicki, Plewa & Różycka (1996); later improvements to the code and test results will be described in detail in Kudlicki et al. (in preparation). *CPPA* employs a three-dimensional Cartesian grid fixed in dimensionless comoving coordinates (see Gnedin 1995). The Poisson equation is solved by a standard FFT-based routine, working on the same grid as the Euler solver. Advection of mass and momenta is done using the piecewise-parabolic scheme, as described by Colella & Woodward (1984). The advection step consists of a series of sweeps along the main axes of the computational domain. Unlike Peebles (1987), we use a variable timestep, according to the CFL condition. To allow for shell crossing on small scales, and inhibit the unrealistically high densities at cluster centres, we artificially interchange fluxes across local directional maxima of the density field. During a sweep, if a local directional maximum of density is encountered, and there is matter falling onto it from both sides, then the fluxes of density and momentum calculated at the left and right interface of the maximum density cell are interchanged. Performed in all directions, it successfully inhibits the non-physical transfer of power into the smallest scales, while conserving the total momentum. We are aware that our code does not reproduce small-scale structures properly, however for the present purpose – involving window functions larger than $3h^{-1}\text{Mpc}$ (Gaussian) and $6h^{-1}\text{Mpc}$ (Top Hat) – it is an efficient and satisfactory tool.

3.2 Selection of the parameters and the models

Since the relation between density and scaled velocity divergence depends very weakly on the background cosmological model (see the previous section), we were free to choose the convenient and well-tested Einstein–de Sitter model ($\Omega = 1, \Lambda = 0$).

To estimate random errors, we have performed six realizations of this cosmological model, each of them with different random phases of the initial density field.

We aimed at investigating the statistics of density and velocity fields on both intermediate (several megaparsecs) and large (up to $60h^{-1}\text{Mpc}$) scales, so, in order to suppress the effects of finite simulation volume size and improve the statistics we decided to make the simulation box significantly larger than the largest filter used. A reasonable solution turned out to be a $(200h^{-1}\text{Mpc})^3$ cube with standard periodic boundary conditions. For 64^3 grid cells, the spatial resolution is $3.125h^{-1}\text{Mpc}$, sufficient for our purposes. As a test we performed a simulation with 128^3 grid cells for a $(200h^{-1}\text{Mpc})^3$ cube and the results remained in good agreement with those obtained with the coarser grid.

Most of the analytical calculations in the discussed regime have been done for scale-free, or power-law, power spectra, $P(k) \propto k^n$. These spectra may seem artificial, none the less they are believed to approximate the real power spectrum at least piecewise over significant ranges of wavelengths. In particular, in the range of scales ~ 1 – $20h^{-1}\text{Mpc}$, the observed power spectrum is well approximated by a power law (e.g., Sutherland et al. 1999; Freudling et al. 1999). That is why we have decided to use a power law power spectrum in our simulations. For convenience, we have picked such normalization of the initial density contrast,

[§] B99 argued however that this result should remain valid for top-hat smoothed fields with vanishing variance.

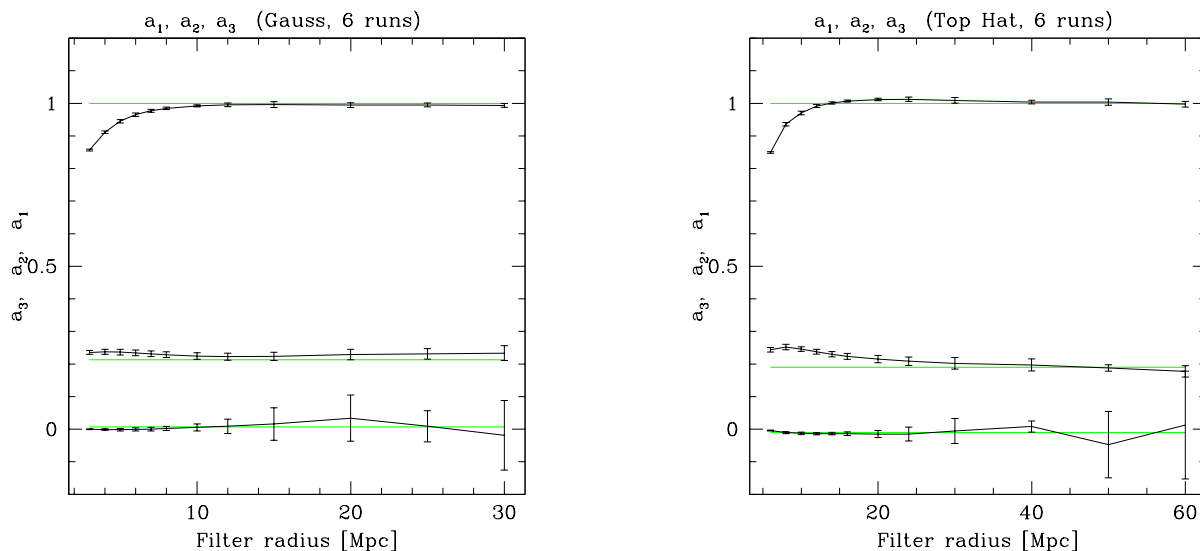


Figure 3. The coefficients a_1, a_2, a_3 from six simulations (curves and error-bars) and their third-order perturbation theory predictions (solid lines). Left panel: Gaussian filter, right panel: Top-Hat filter.

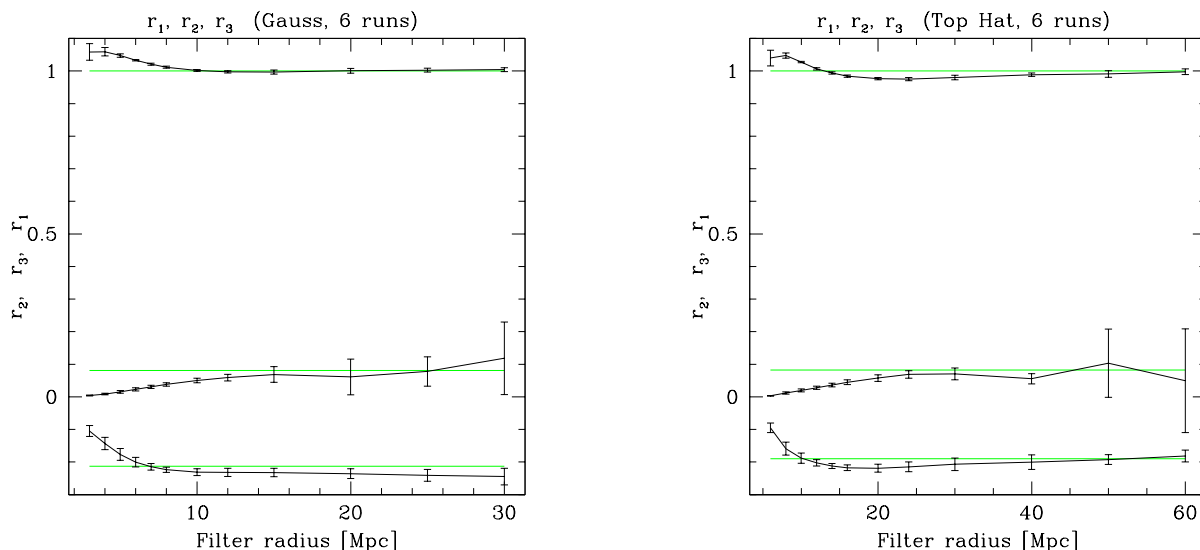


Figure 4. The coefficients r_1, r_2, r_3 from six simulations (curves and error-bars) and their third-order perturbation theory predictions (solid lines). Left panel: Gaussian filter, right panel: Top-Hat filter.

that the amplitude of the linear growing mode measured with a $8h^{-1}\text{Mpc}$ top-hat filter at present epoch is unity, $(1 + z_{\text{initial}})\sigma_{8,\text{initial}} = 1$. Since we have chosen a scale-free power spectrum, the results may be simply rescaled to other normalizations.

Observations suggest that on mildly non-linear scales the effective spectral index n lies between -1 and -1.5 (Baugh & Efstathiou 1993, 1994; Fisher et al. 1993; Feldman et al. 1994; Park et al. 1994; Lin et al. 1996; Sutherland et al. 1999). For our simulations we have chosen the value of $n = -1$, because one of our code tests was to compare the PDF of the velocity divergence with the analytical formula of Bernardeau (1994). This comparison was essential to demonstrate the advantage of our code over N-body simulations in *velocity* field studies.

N-body schemes yield mass-weighted velocity fields, re-

sulting in spurious velocity gradients. These gradients manifest themselves as spurious tails in the PDF of θ . Tessellation techniques, invented by Bernardeau & van de Weygaert (1996) to overcome this problem, are very CPU-time-consuming, and the results have much lower resolution than the simulations themselves. (Commonly 50^3 compared to 128^3 : Bernardeau & van de Weygaert 1996; Bernardeau et al. 1997; B99). In contrast, our code yields directly a volume-weighted velocity field. Figure 2 presents the comparison of the PDF of θ as recovered from our numerical data with the analytical formula of Bernardeau (1994). The velocity field is smoothed with a top-hat filter of the radius of $8h^{-1}\text{Mpc}$. Note that the PDF obtained from the simulations has no spurious tails, whatsoever. The definition of the scaled divergence is such that negative θ corresponds to positive divergence, i.e., to the expansion of voids. Note how well the

negative tail of our PDF traces the analytical prediction, on over three decades of the probability value. (Compare Fig. 6 of Bernardeau 1994.) In the extreme part of the positive tail, the analytical PDF slightly overestimates the measured one. This is to be expected, since the formula of Bernardeau (1994) is only an approximate fit to the actual PDF, overestimating the value of skewness of the distribution (2 instead of 1.7 based on PT). Indeed, in our simulations the skewness measured with an $8 \text{ h}^{-1}\text{Mpc}$ top-hat filter has the value of 1.77 ± 0.11 .

4 THE FORWARD RELATION

With our models, we have tested the polynomial approximation of the mean forward DVDR (Eq. 4).

We compare the coefficients a_1, a_2 and a_3 computed from our simulations to the corresponding third-order PT values in Figure 3. These coefficients have been computed from the simulations using a standard four-parameter[¶] least square fit on data from each of the 64^3 grid cells (after smoothing with the filters required). We have also performed a fit for all the coefficients a_0 through a_5 , in this case a_4 and a_5 were consistent with zero, and the values of $a_0 \dots a_3$ did not change remarkably between these two fits. With the exception of the most highly non-linear smoothing scales, the values of a_n very weakly depend on the filter size, and are in good agreement with the perturbation theory predictions of CL97.

5 THE INVERSE RELATION

5.1 Polynomial parameterization

As we have shown above, the mean forward relation can be described with sufficient accuracy by the polynomial formula (4) on the relevant scales. In this section we test the polynomial approximation (5) to the inverse relation.

In Fig. 4 we present our numerical estimates of the parameters r_1, r_2 and r_3 . On scales below $\sim 8 \text{ Mpc}$ for Gaussian and $\sim 15 \text{ Mpc}$ for top-hat filtering, their dependence on the filter size is very strong, especially for r_2 , which is the first, and therefore the most essential parameter describing the non-linearity of the DVDR. This makes the polynomial formula inconvenient for application to observational data. Even using the value of r_2 predicted for a particular filter size will not help much since all sizes scale with the present-epoch density contrast, σ_8 , and the Hubble constant, h , and neither of these parameters is known accurately yet.

We have also performed a fit for the parameters r_0 through r_5 of the fifth-order polynomial in δ . The values of r_4 and r_5 turn out to be inconsistent with zero at more than 2σ level for filter sizes smaller than $20 \text{ h}^{-1}\text{Mpc}$, and, which is still more important, their addition to the fit significantly influences r_1, r_2 and r_3 (see Figure 5). Moreover, a third-order polynomial that fits the distribution in the large-scale regime (for small $|\delta|$) obviously has a non-monotonic

[¶] We have found that the value of a_0 is perfectly consistent with $-a_2\sigma_\theta^2$, and that a 3-parameter fit with the $a_0 = -a_2\sigma_\theta^2$ constraint gives the same values for a_1, a_2 and a_3 .

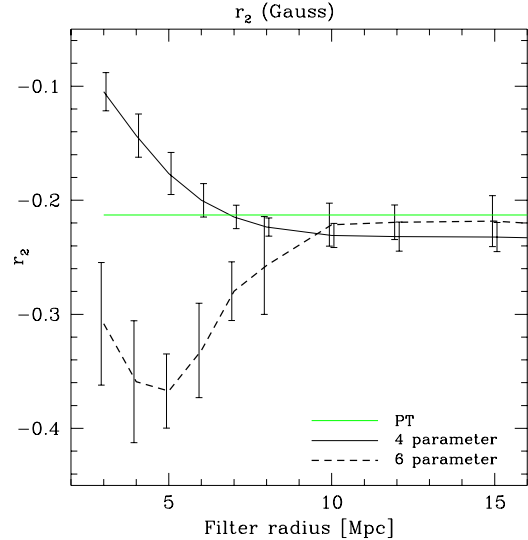


Figure 5. The value of r_2 from 4-parameter fit (thin solid curve) and 6-parameter fit (dashed curve). Heavy solid line represents the third-order perturbation theory value.

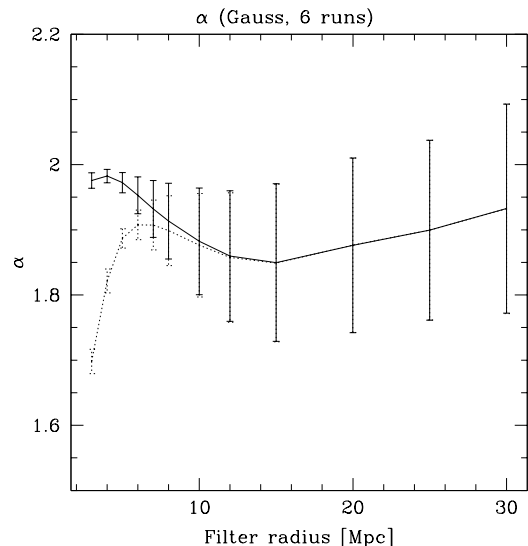


Figure 6. The α parameter of the $\langle\theta_\delta\rangle$ relation. Dotted curve and error-bars: fit with second-order approximation to ϵ ; solid: α from fit of both α and ϵ .

derivative, which is inconsistent with the properties of the actual distribution. Figure 1 clearly demonstrates that the first derivative of the relation is positive and monotonically decreasing. The third-order polynomial fit to the simulated data is drawn with a long-dashed line in Figure 7. One can observe that this function has an inflection point well within the range of δ and θ occupied by numerical data, not seen in the simulated relation. Another substantial disadvantage of high-order polynomial fits is the high number of parameters, each of them depending on the smoothing scale. Finally, the r_n parameters are strongly correlated, so possibly another formula, dependent on fewer parameters and not a polynomial, will provide a better description.

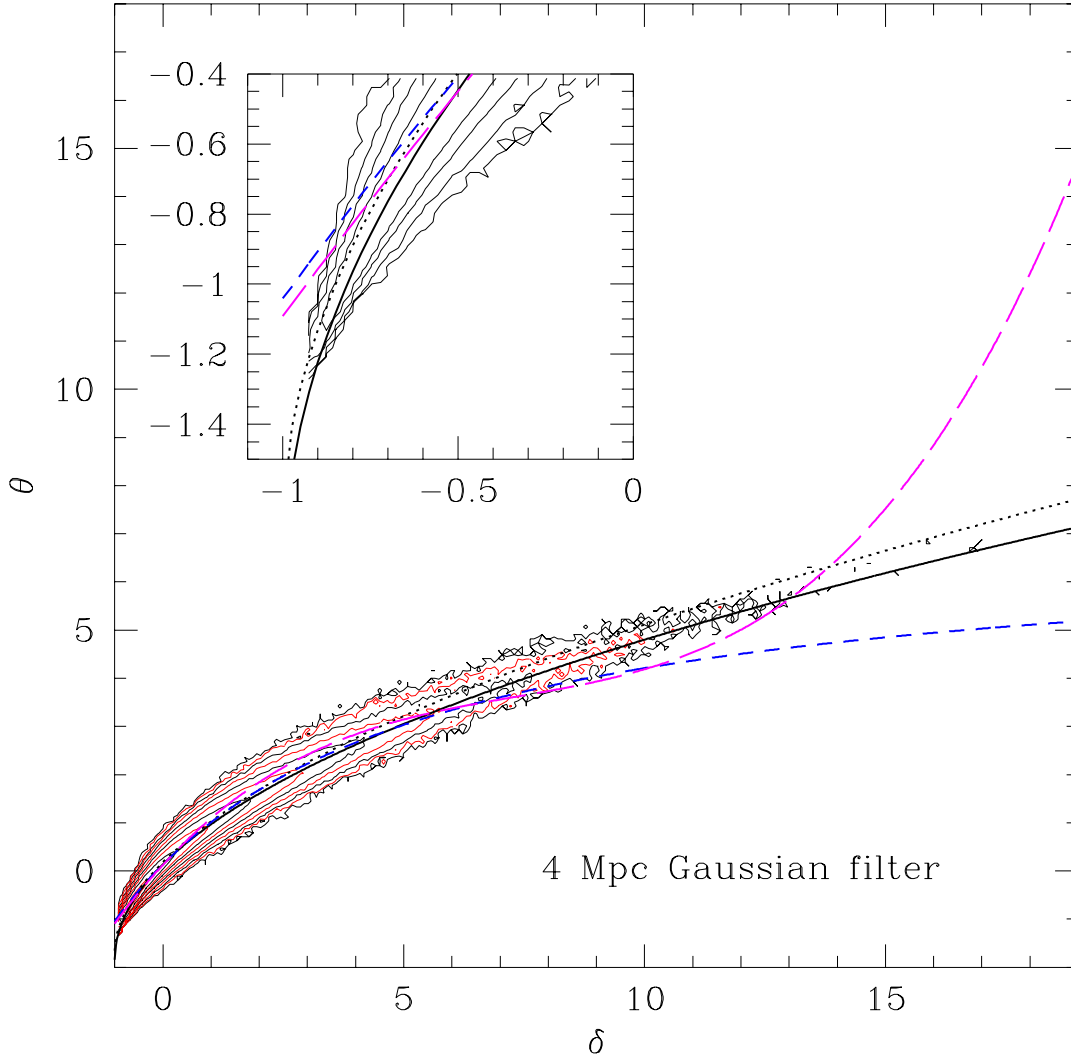


Figure 7. Joint PDF of δ and θ , $P(\delta, \theta)$: contours have intervals of 0.5 in $\log_{10}(P)$; combined data from six simulations are plotted. Solid curve represents our formula (7) with α and ϵ fitted independently, dotted curve – a one-parameter fit according to formula (7) with the ϵ offset accurate to the second order (eq. 8). Long-dashed curve represents the third-order polynomial fit (5), and short-dashed – the non-linear formula of Willick et al. (1997). Window in the upper-left corner enlarges the void region, here for clarity contours have intervals of 1.0 in $\log_{10}(P)$.

5.2 A robust non-linear formula

In search for a better formula for the $\langle \theta | \delta \rangle$ relation one needs to take into account: (a) monotonicity of the fit and its derivative, (b) agreement with the polynomial description for large filter radii, (c) proper asymptotic behavior in the voids, and (d) the mass conservation law, i.e. the formula should yield $\langle \theta \rangle = 0$. Of the above, (a), (b) and (c) are satisfied by the asymptotic formula of Bernardeau (1992), (see eq. 6 of this paper), which was derived in the limit of zero density dispersion, $\sigma_\delta \rightarrow 0$, and which does not account for smoothing effects. Filtering of the data substantially affects the higher order moments of the distribution of δ and θ , and therefore it is expected to cause a change in the shape of the DVDR. In order to make equation (6) applicable to filtered data (and such are all the data obtained from galaxy

catalogs) we have made an educated guess, replacing the exponent of $2/3$ in the formula with a free parameter, $1/\alpha$.^{||} This change does not affect the shape of the fit in the void wing of the plot, as long as α is not very much different from $\frac{3}{2}$. To satisfy (d), i.e. to keep the average θ equal zero, we add a constant, depending only on α and scaled by the density dispersion. Our final formula has the form:

$$\theta = \alpha [(1 + \delta)^{1/\alpha} - 1] + \epsilon, \quad (7)$$

where the constant ϵ can be approximated as:

^{||} This follows the idea of B99 in a sense, but will result in a much simpler formula.

$$\epsilon = \frac{\alpha - 1}{2\alpha} \sigma_\delta^2. \quad (8)$$

Formula (8) is accurate to the second order, we have tested its relevance by fitting both α and ϵ as independent parameters. The values of α obtained in these two fits are consistent for filter radii larger than about $6h^{-1}\text{Mpc}$ (see Figure 6).

We plot the joint PDF of δ and θ combined from all our six simulations in Figure 7. Willick & Strauss (1998) performed their VELMOD analysis of peculiar velocities using IRAS galaxy density field convolved with either $3h^{-1}\text{Mpc}$ or $5h^{-1}\text{Mpc}$ Gaussian filter. They reported very similar results for both smoothing scales. Therefore, we chose to plot the distribution for data filtered with $4h^{-1}\text{Mpc}$ Gaussian kernel.

Formula (7) is drawn in this figure with heavy solid line (two-parameter fit), and dotted line (one-parameter fit, offset accurate to the second order, formula 8). The long- and short-dashed lines represent respectively the third-order polynomial fit and a formula by Willick et al. (1997):

$$\langle \theta | \delta \rangle = \frac{(1 + a^2 \sigma_\delta^2) \delta + a \sigma_\delta^2}{1 + a \delta}, \quad (9)$$

in which a is a free parameter. The polynomial fit is poor not only for very large δ , but it also overestimates θ for $1 < \delta < 5$. The formula of Willick et al. follows the PDF as closely as ours for $-0.6 < \delta < 4$, but departs from the simulated distribution at the extreme values of δ . We have also estimated a from our simulations, obtaining the value of 0.14 at the $4h^{-1}\text{Mpc}$ scale. At large scales our estimate of a is rather 0.24 than 0.28 reported by Willick et al.

Our fit for the one-parameter α -formula slightly overestimates θ in the high- δ tail. With the two-parameter description used instead, our formula fits the data very well in the entire range of δ , at a slightly greater α .

The weak dependence of α on the smoothing scale is well visible in Figure 6 (in the two-parameter description, $\alpha \simeq 1.9 \pm 0.1$). As stated earlier, the formula (7) as a description of the inverse relation was our ‘educated’ guess. Expanding it for large smoothing scales, and comparing it with the polynomial description we find that $\alpha \simeq \alpha_{LS} = 1/(1 + 2r_2)$. From Figure 4 we obtain $\alpha_{LS} \simeq 1.95$, which remains in good agreement with direct fit. For very small smoothing scales, simple considerations of energy conservation in the model of spherical collapse yield $\alpha = 2$. We expect α to change very weakly between weakly and highly non-linear scales, which is indeed observed.

Our formula is also much simpler than formula (18) of B99 for the forward relation. The reason that the formula of B99 is complex is twofold. Firstly, B99 aimed at modelling the weak Ω -dependence of the relation. However, the Ω -dependence turned out to be so weak that it was practically unnecessary to account for it. Secondly, they rigorously applied the constraint, coming from the maximal expansion of voids, that $\theta = -3/2$ for $\delta = -1$. Although we have not required it explicitly, our formula satisfies this ‘voids’ constraint very well (see Fig. 7).

6 SUMMARY AND CONCLUSIONS

We have tested several parameterizations of the density vs. velocity divergence relation on weakly and mildly non-linear scales. We confirm that the polynomial formula provides a

good description for the forward relation (the density contrast as a function of the velocity divergence).

On the other hand, the inverse relation is not well described by the polynomial expansion, which does not converge fast enough. Also, on mildly non-linear scales the parameters of the expansion strongly depend on the smoothing scale. The formula of Willick et al. (1997) is better than the polynomial description, but it is not free from drawbacks, either. Firstly, for large densities it has a horizontal asymptote, not observed in the simulated distribution. As a result, in the high-density tail it underestimates the actual relation. Secondly, like the polynomial description, it incorrectly describes the low-density tail (i.e., the relation for voids).

Our formula (7) is free from these disadvantages. It is also simpler (in its simplest form it depends on one parameter only), which makes it easy to implement in the velocity-velocity comparisons.

ACKNOWLEDGMENTS

This work was supported by the KBN grant 2P-03D-004-13. The simulations are partly performed at the *Interdisciplinary Centre for Mathematical and Computational Modelling* in Warsaw.

REFERENCES

- Bardeen J., Bond J. R., Kaiser N., Szalay A., 1986, *ApJ*, 304, 15
 Baugh, C. M. and Efstathiou, G., 1993 *MNRAS* 265, 145
 Baugh, C. M. and Efstathiou, G., 1994 *MNRAS* 267, 323
 Bernardeau F., 1992, *ApJ*, 390, L61
 Bernardeau F., 1994, *A&A*, 291, 697
 Bernardeau F., van de Weygaert R., 1996, *MNRAS*, 279, 693
 Bernardeau F., van de Weygaert R., Hivon, E. and Bouchet, F. R., 1997 *MNRAS* 290, 566
 Bernardeau F., Chodorowski, M. J., Lokas, E. L., Stompor, R. and Kudlicki, A., 1999 preprint astro-ph/9901057 (B99)
 Blanton M., Cen R., Ostriker J. P., Strauss M. A., 1998, astro-ph/9807029
 Catelan P., Lucchin F., Matarrese S., Moscardini L., 1995, *MNRAS*, 276, 39
 Cen R., Ostriker J. P., 1992, *ApJ*, 399, L113
 Chodorowski, M. 1997, *MNRAS* 292, 695
 Chodorowski M. J. and Lokas E. L., 1997, *MNRAS*, 287, 591 (CL97)
 Chodorowski, M., Lokas, E. L., Pollo, A. and Nusser, A., 1998, *MNRAS* 300, 1027 (CLPN)
 Colella, P., and Woodward, P.R., 1984, *J. Comput. Phys.*, 54, 174
 da Costa L. N. et al. 1998, *MNRAS*, 299, 425
 Davis M., Geller M. J., 1976, *ApJ*, 208, 13
 Davis M., Efstathiou G., Frenk C. S., White S. D. M., 1985, *ApJ*, 292, 371
 Davis M., Nusser A. & Willick J. A. 1996, *ApJ*, 473, 22
 Dressler A., 1980, *ApJ*, 236, 351
 Dekel A., Silk J., 1986, *ApJ*, 303, 39
 Dekel A., Bertschinger E., Yahil A., Strauss M.A., Davis M., Huchra J. P., 1993, *ApJ*, 412, 1
 Dekel A., Lahav O., 1998, astro-ph/9806193
 Feldman, H. A., Kaiser, N. and Peacock, J. A., 1994 *ApJ* 426, 23
 Fisher K. B., Davis, M., Strauss, M. A., Yahil, A. and Huchra, J. P., 1993 *ApJ* 402, 42
 Fisher K. B. et al. 1995, *ApJS*, 100, 69
 Freudling W., et al., 1999, preprint astro-ph/9904118

- Ganon G., Dekel A., Mancinelli P. J., Yahil A., 1999, in preparation
- Giovanelli R., Haynes M. P., Chincarini G. L., 1986, *ApJ*, 300, 77
- Gnedin N.Y., 1995, *Astrophys. J. Suppl. Ser.*, 97, 231
- Gramann M., 1993, *ApJ*, 405, L47
- Guzzo L., Strauss M. A., Fisher K. B., Giovanelli R., Haynes M. P., 1997, *ApJ*, 489, 37
- Hermit S., Santiago B. X., Lahav O., Strauss M. A., Davis M., Dressler A., Huchra J. P., 1996, *MNRAS*, 283, 709
- Hudson M. J., Dekel A., Courteau S., Faber S. M., Willick J. A., 1994, AAS meeting, 185, 119
- Kaiser N., 1984, *ApJL*, 284, L9
- Kauffman G., Nusser A., Steinmetz M., 1997, *MNRAS*, 286, 795
- Kudlicki A., Plewa T., Różycka M., 1996, *A.A.* 46, 297
- Kudlicki A., et al., 1999, in preparation
- Lahav O., Lilje P. B., Primack J. R., Rees M. J., 1991, *MNRAS*, 251, 128
- Lin, H., Kirshner, R. P., Shectman, S. A., Landy, S. D., Oemler, A., Tucker, D. L. and Schechter, P. L., 1996 *ApJ*, 471, 617
- Loveday J., Efstathiou G., Maddox S. J., Peterson B. A., 1996, *ApJ*, 468, 1
- Mancinelli P. J., Yahil A., Ganon G., Dekel A., 1994, in Bouchet F. R., Lachièze-Rey M., eds, *Proc. 9th IAP Astrophysics Meeting, Cosmic Velocity Fields*. Editions Frontières, Gif-sur-Yvette, p. 215
- Mancinelli P. J., Yahil A., 1995, *ApJ*, 452, 75
- Nusser A., Dekel A., Bertschinger E., Blumenthal G. R., 1991, *ApJ*, 379, 6
- Park, C., Vogeley, M. S., Geller, M. J. and Huchra, J. P., 1994 *ApJ* 431, 569
- Peebles, P. J. E., 1987, *ApJ* 317, 576
- Riess A. G., Davis M., Baker J., Kirshner R. P., 1997, *ApJ*, 488, L1
- Santiago B. X., Strauss M. A., 1992, *ApJ*, 387, 9
- Sigad Y., Eldar A., Dekel A., Strauss M. A., Yahil A. 1998, *ApJ*, 495, 516
- Sutherland W., et al., 1999, preprint astro-ph/9901189
- Tegmark M., Bromley B. C., 1998, astro-ph/9809324
- Willick J. A. et al. 1997, *ApJS*, 109, 333
- Willick J. A. and Strauss, M. A. 1998, *ApJ* 507, 64
- Willick J. A., Strauss, M. A., Dekel, A. and Kolatt, T. 1997, *ApJ*, 486, 629